Theoretical Studies of Simple Polar Fluids

Stenhammar, Joakim

2012

Document Version:
Publisher's PDF, also known as Version of record

Theoretical Studies of Simple Polar Fluids

Joakim Stenhammar

Division of Physical Chemistry
Lund University, Sweden

LUND UNIVERSITY

Doctoral Thesis in Physical Chemistry

The thesis will be publicly defended at 10.30 on Friday the 3rd of February, 2012 in lecture hall B, Kemicentrum.

The faculty opponent is Professor Martin Neumann, Universität Wien, Austria.

Division of Physical Chemistry
Lund University
P.O. Box 124
SE–221 00 Lund
Sweden

ISBN 978-91-7422-287-6
Printed by Media-Tryck, Lund University

Organization	Document name
Lund University	Doctoral dissertation
	Date of issue: February 3, 2012
Author(s): Joakim Stenhammar	Sponsoring organization: Swedish Research Council (VR)

Title and subtitle: Theoretical Studies of Simple Polar Fluids

Abstract

Fluids composed of dipolar molecules are ubiquitous in nature, with water being the most prominent example. Due to their great importance and large complexity, a basic scientific understanding of the structure and thermodynamics of polar fluids is essential. In this thesis, simple polar model fluids are investigated with the aim of adding a bit to this understanding. In particular, the topics addressed include:

- Electrostatic fluctuations in polar fluids, in bulk as well as under confinement.
- van der Waals interactions between spherical bodies composed of permanent dipoles.
- Schemes for handling finite-size effects in computer simulations of polar fluids.

In most of the studies, two different model systems are investigated, namely (i) a dielectric continuum model, solved using analytical techniques, and (ii) a discrete point-dipole ("Stockmayer") model, solved using molecular simulations. Thus, an additional prospect of the studies is to assess the accuracy of the dielectric continuum approximation in different contexts.

Key words	
Polar fluids, Dielectric theory, van der Waals forces, Molecular simulation	
Classification system and/or index terms (if any)	
Supplementary bibliographical information	Language: English
ISSN and key title	ISBN: 978-91-7422-287-6
Recipient's notes	Number of pages: 146 / Price / Security classification

Distribution by (name and address)

LIST OF PAPERS

This thesis is based on the following papers, which will be referred to in the text by their Roman numerals. The papers are appended at the end of the thesis.

I **Electric multipole moment fluctuations in polar liquids**
Joakim Stenhammar, Per Linse, Per-Åke Malmqvist, and Gunnar Karlström (2009)
The Journal of Chemical Physics, **130**, 124521.

II **A unified treatment of polar solvation using electrostatic fluctuations**
Joakim Stenhammar, Per Linse, and Gunnar Karlström (2011)
Chemical Physics Letters, **501**, 364–368.

III **Anisotropic electric fluctuations in polar liquids under spherical confinement**
Joakim Stenhammar, Per Linse, and Gunnar Karlström (2011)
Molecular Physics, **109**, 11–20.

IV **An exact calculation of the van der Waals interaction between two spheres of classical dipolar fluid**
Joakim Stenhammar, Per Linse, Håkan Wennerström, and Gunnar Karlström (2010)
The Journal of Physical Chemistry B, **114**, 13372–13380.

V **Classical van der Waals interactions between spherical bodies of dipolar fluid**
Joakim Stenhammar and Martin Trulsson (2011)
Physical Review E, **84**, 011117.

VI **Nondielectric long-range solvation of polar liquids in cubic symmetry**
Joakim Stenhammar, Per Linse, and Gunnar Karlström (2009)
The Journal of Chemical Physics, **131**, 164507.

VII **Structural anisotropy in polar fluids subjected to periodic boundary conditions**
Joakim Stenhammar, Per Linse, and Gunnar Karlström (2011)
Journal of Chemical Theory and Computation, in press.

VIII **Bulk simulation of polar liquids in spherical symmetry**
Joakim Stenhammar, Per Linse, and Gunnar Karlström (2010)
The Journal of Chemical Physics, **132**, 104507.

List of Contributions

I I performed the study and was responsible for writing the paper.

II I performed the study and was responsible for writing the paper.

III I performed the study and was responsible for writing the paper.

IV I performed the study and was responsible for writing the paper.

V I performed the final study and was responsible for writing the paper.

VI I performed the study and was responsible for writing the paper.

VII I performed the study and was responsible for writing the paper.

VIII I performed the study and was responsible for writing the paper.

Other Papers, Not Included in the Thesis

- **Effects of different boundary conditions on the long-range structure of polar liquids**
  Gunnar Karlström, Joakim Stenhammar, and Per Linse (2008)
  Journal of Physics: Condensed Matter, **20**, 494204.

- **Some comments and corrections regarding the calculation of electrostatic potential derivatives using the Ewald summation technique**
  Joakim Stenhammar, Martin Trulsson, and Per Linse (2011)
  The Journal of Chemical Physics, **134**, 224104.

PREFACE

This thesis contains most of the scientific results from my four and a half years as a PhD student at Physical Chemistry (1). It is organized in the standard way, starting with a relatively short overview of the basic scientific problems and the methods used to solve them. The results are contained in the eight journal papers appended at the end of the thesis, although a short summary of the main findings is also given in Chapter 5.

During the course of my thesis work I have encountered many helpful people, some without whom this book would never have been written. The first, and all-overshadowing, acknowledgement of course goes to my supervisors **Per** and **Gunnar** for always being generous with their time and knowledge on scientific as well as non-scientific issues; it has been a true pleasure to work together with you! I would also like to thank **Martin** for a very fruitful collaboration, and I really hope there will be more to come in the future! The enlightening discussions with **Christoffer**, **Håkan**, **Luís**, and **Per-Åke**, which have provided me with important scientific insights are kindly acknowledged. Furthermore, I would like to thank **Magnus** for computer support and **Frans** and **Johanna** for reading and providing feedback on my thesis. Last, but definitely not least, I would like to thank everyone at the divisions of **Physical and Theoretical Chemistry** ("ingen nämnd, ingen glömd") for the many interesting, mostly highly non-scientific discussions over lunch, coffee, and beer, that have helped making my four years at the department so enjoyable!

Lund, November 2011
J.S.

"Be nice to nerds. Chances are you'll end up working for one."
— Bill Gates

CONTENTS

POPULÄRVETENSKAPLIG SAMMANFATTNING

Att vatten, H_2O, är en otroligt viktig vätska för allt liv på jorden känner de flesta till; exempelvis består över hälften av människokroppen av vatten, och 70 procent av jordens yta är täckt av det. Att just denna till synes enkla kemikalie, vars molekyler består av två väteatomer och en syreatom, har en sådan unik betydelse är ingen slump, utan beror på att vatten har en rad mycket unika egenskaper som andra vätskor saknar. Exempelvis är vatten i fast form (is) lättare än i flytande form, vilket gör att våra sjöar och hav fryser uppifrån istället för från botten, vilket hade varit förödande för allt vattenliv. En del, om än långtifrån alla, av vattens unika egenskaper kan förklaras utifrån vattenmolekylens geometriska form. Vattenmolekylen är nämligen vinklad (V-formad), med syreatomen i ”hörnet” och en väteatom i varje ände. Eftersom syreatomen har en större förmåga att dra till sig negativt laddade elektroner än vad väteatomerna har får vattenmolekylen en positivt laddad och en negativt laddad ände; vi säger att vattenmolekylen är en *dipol*, och att vatten är en *polär vätska*. En molekyls dipol brukar åskådliggöras med en pil (”vektor”) som pekar från dess negativa till dess positiva ände. I Figur 1 syns en vattenmolekyl med sin dipolvektor som pekar från ”syreänden” till ”väteänden”.

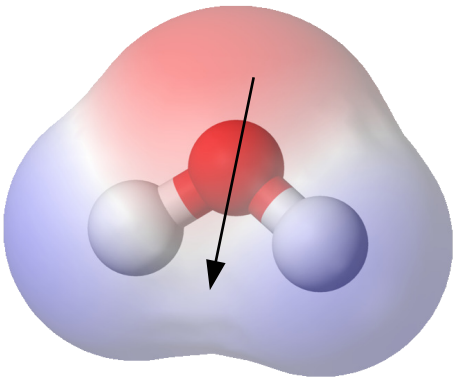

Figur 1: En vattenmolekyl med en tredimensionell karta över sin laddningsfördelning; röda områden är negativt laddade (många elektroner), medan blåa områden är positivt laddade (få elektroner). Pilen visar riktningen, från den negativa till den positiva änden, på vattenmolekylens dipol.

Eftersom vatten är ett så viktigt och samtidigt komplext ämne har ofantliga mängder forskning ägnats åt att undersöka dess egenskaper. En stor del av denna forskning har använt sig av experimentella tekniker, men eftersom molekyler är väldigt små (ett glas vatten innehåller sisådär 10 000 000 000 000 000 000 000 000 000 molekyler!) och rör sig fort är det svårt att få detaljerad information från ett experiment om vad som händer på molekylär nivå. Därför har mycket forskning ägnats åt att bygga teoretiska modeller som kan beskriva vad som sker på molekylnivån, oftast med hjälp av beräkningar i dator. Även om moderna datorer är förhållandevis snabba krävs oundvikligen att man gör förenklingar av verkligheten när man konstruerar sådana modeller för att kunna få fram den information man vill åt inom rimlig tid. En sådan förenkling är att ignorera vattenmolekylens vinklade form, och ersätta dess tre atomer med endast en atom, i vars centrum man ”bäddar in” en dipol. Denna förenkling gör att datorberäkningen går minst tio gånger snabbare, samtidigt som man såklart förlorar en del av egenskaperna hos den verkliga vattenmolekylen. En ytterligare förenkling av verkligheten kan vi åstadkomma genom att helt sonika ta bort vattenmolekylerna helt och hållet, och istället ersätta dem med en slät, utsmetad ”bakgrund” med en dipol*täthet*. Detta är uppenbart en väldigt grov förenkling av verkligheten, men i gengäld är sådana modeller i allmänhet relativt enkla att hantera; oftast behövs inte ens datorer till hjälp, utan ekvationerna kan lösas med papper och penna. I Figur 2 visas en schematisk bild på ”verkligt” vatten samt dessa två förenklade modeller.

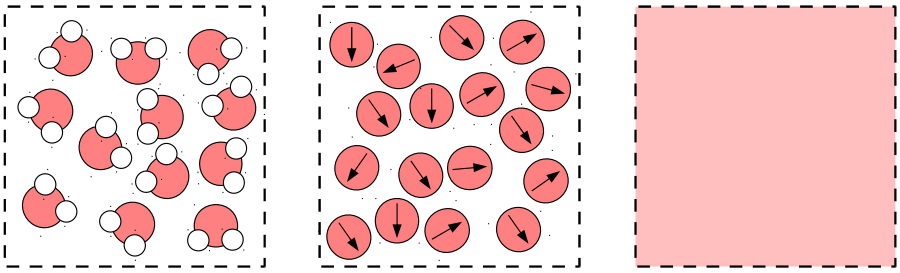

Figur 2: Tre olika modeller för att beskriva vatten. Från vänster: ”Molekylärt vatten”, med två väte- och en syreatom per molekyl, ”sfäriskt vatten”, där de tre atomerna ersatts av en enda atom med en dipol inbäddad i centrum, samt en ”utsmetad” vattenmodell, där molekylerna ersatts med en uniform bakgrund beskriven av en dipoltäthet.

I min avhandling har jag använt mig av dessa två förenklade modeller för att studera grundläggande egenskaper hos polära vätskor. Bland annat har jag försökt besvara följande frågor:

- Hur beter sig molekylerna i en polär vätska nära en yta, i till exempel ett glas vatten, jämfört med långt ifrån ytan?
- Hur stor är den attraktiva kraften mellan två droppar av polär vätska, beroende på deras separation?
- Hur kan vi bära oss åt för att snabba upp och på andra sätt förbättra datorberäkningarna när vi vill studera olika vätskemodeller?

Förhoppningsvis kan min forskning bidra med en liten del till den grundläggande förståelsen av polära vätskor i allmänhet och vatten i synnerhet.

CHAPTER

ONE

INTRODUCTION

Fluids composed of dipolar molecules or particles are common in nature, ranging from seemingly simple molecular fluids to complex macromolecular suspensions and solutions. The by far most important example of a dipolar fluid is water, due to its huge abundance and peculiar properties. For this reason, tremendous amounts of research [1–3], as well as a fair share of pseudoscience [4–8], have been devoted to the study of the basic structural, dynamical and thermodynamic properties of water. Most of the studies done on "generic" polar fluids, i.e. polar fluids not exhibiting the many thermodynamic anomalies of water, have considered models that combine the anisotropic dipole–dipole potential with a hard ("dipolar hard spheres") or a soft ("dipolar soft spheres") repulsion, and sometimes also with a short-range isotropic attraction ("Stockmayer particles"). A lot of effort has been put into understanding the liquid-vapor phase coexistence [9], the dielectric properties [10] and the behavior under confinement [11] of these relatively simple model fluids.

One explanation to why polar fluids have been studied extensively is that they are structurally and thermodynamically more complex than one might first expect. One reason behind this is the formally infinite range of the dipole–dipole potential, implying that the local structure in one part of the fluid depends on the local structure in very distant regions. Needless to say, this poses large technical difficulties when trying to simulate dipolar systems in computers that can only handle, from a thermodynamic perspective, very few particles. Thus, elaborate schemes [12] have been developed to artificially emulate an infinite system, while explicitly handling only a finite-sized one. Alternatively, the finite-size problem can be avoided either by using approximate analytical techniques [10] that allow for properly approaching the

thermodynamic limit, or by using dielectric continuum theory [13], where discrete particles are replaced by a structureless, smeared out dipolar density described by its relative dielectric permittivity. This seemingly radical approximation has been shown to be surprisingly successful in describing many physical situations where polar fluids, in particular water, are involved [14], in spite of the fact that all structural information is lost when moving to the continuum description.

In this thesis, a number of basic problems involving polar fluids will be investigated. The studies included in the thesis can roughly be categorized into three sections:

- **Development of expressions describing the magnitude of electrostatic fluctuations in dipolar fluids.** In Paper I, expressions describing the electrostatic fluctuations in an infinite fluid in terms of its multipole moments are developed and tested, and in Paper II they are used to analyze the solvation free energy of a sub-volume inside an infinite fluid sample. In Paper III, the corresponding fluctuation formulas for the case of a spherically confined fluid are derived and tested towards computer simulation results.

- **Investigation of the van der Waals interaction between spherical bodies of dipoles.** In Paper IV, a dielectric model is used to describe the separation-dependent free energy of interaction between two spherical bodies composed of permanent dipoles. In Paper V, the continuum results are compared to results from a model using discrete particles.

- **Investigation of schemes for finite-size corrections in computer simulations.** In Paper VI, the fluctuation formulas derived in Paper I are used to investigate the effect of using periodic boundary conditions to handle dipole–dipole interactions. In Paper VII, this analysis is extended through the development of a quantitative dielectric model describing the polarization coming from the periodic boundaries. Finally, in Paper VIII, an alternative scheme, so-called image boundary conditions, for treating long-range interactions is examined.

For all these studies, two different models were used, namely (*i*) a dielectric continuum description which was used to derive analytical expressions, and (*ii*) a discrete Stockmayer fluid model, solved using computer simulation methods. Generally, the Stockmayer fluid served as the simplest possible benchmark system against which to test the dielectric expressions. Thus, an additional motivation behind all of the studies listed above was to assess the validity of the dielectric approximation in various contexts.

CHAPTER
TWO

ELECTROSTATIC INTERACTIONS

The subject of electrostatics seeks to describe the interaction between and behavior of stationary or slowly moving charged objects. In the following chapter, we will introduce the concept of multipole expansions, and apply it to the electrostatic interaction between two molecules in vacuum, focusing in particular on the interaction between two ideal dipoles (Section 2.1). The concept of dipolar interactions will then be extended to angle-averaged interactions (Section 2.2) and dielectric continuum theory (Sections 2.3 – 2.4). Most of the theory contained in this chapter can be found in standard textbooks; for accessible expositions, the books by Evans and Wennerström [14] and Israelachvili [15] are recommended, whereas more rigorous treatments are given in the monographs by Griffiths [16] and Jackson [17].

2.1 The interaction between two molecules

One of the basic equations of classical electrostatics is Coulomb's law, which describes the electrostatic force acting between two charged particles as a function of their separation. In its potential form, it reads

$$u_{q_1 q_2} = \frac{q_1 q_2}{4\pi\varepsilon_0 r_{12}}, \tag{2.1}$$

where $u_{q_1 q_2}$ is the electrostatic interaction potential, q_1 and q_2 are the two charges, r_{12} is their separation, and ε_0 is the permittivity of free space. Since q_1 and q_2 can have both positive and negative signs, $u_{q_1 q_2}$ can be both attractive ($u_{q_1 q_2} < 0$) and repulsive ($u_{q_1 q_2} > 0$) depending on whether q_1 and q_2 have equal or opposite signs.

Equation (2.1) is applicable to the interaction between two point charges, i.e. two infinitely small charged particles, which is a relevant model for simple ions. It can, however, readily be generalized to the case of continuous charge distributions, representing for example molecules of arbitrary shape. To this end, we replace the point charges q_1 and q_2 by the charge distributions $\rho_1(\mathbf{r}_1)$ and $\rho_2(\mathbf{r}_2)$ (see Figure 2.1). $\rho(\mathbf{r})$ describes the magnitude and sign of the charge located in a small volume around the point $\mathbf{r}$. The total interaction energy, corresponding to Eq. (2.1), is then given by the interaction between each volume element in ρ_1 and each volume element in ρ_2, i.e.

$$u_{\rho_1\rho_2} = \frac{1}{4\pi\varepsilon_0} \iint \frac{\rho_1(\mathbf{r}_1)\rho_2(\mathbf{r}_2)}{|\mathbf{r}_1 - \mathbf{r}_2|} d\mathbf{r}_1 d\mathbf{r}_2, \tag{2.2}$$

where the integrations over $\mathbf{r}_1$ and $\mathbf{r}_2$ run over all points in ρ_1 and ρ_2, respectively. Equation 2.2 can be used to numerically calculate the electrostatic interaction between two molecules at a fixed orientation, where $\rho(\mathbf{r})$ can be obtained from, for example, a quantum-chemical calculation.

A somewhat more instructive way to use Eq. (2.2) is to expand the separation dependent part $|\mathbf{r}_1 - \mathbf{r}_2|^{-1}$ as an infinite double sum of terms exhibiting a progressively stronger distance dependence:

$$u_{\rho_1\rho_2} = \sum_{\ell_1=0}^{\infty} \sum_{\ell_2=0}^{\infty} \frac{b_{\ell_1\ell_2}(\Omega_{12})}{R_{12}^{\ell_1+\ell_2+1}}, \tag{2.3}$$

where R_{12} is the distance between two arbitrary origins inside ρ_1 and ρ_2, respectively, and the expansion coefficients $b_{\ell_1\ell_2}(\Omega_{12})$ are products of an orientation dependent function and the so-called *multipole moments* of the charge distributions. These can be defined in various ways, and the detailed derivation of the coefficients will not be treated here. We can, however, identify the leading-order term ($\ell_1 = \ell_2 = 0$), with the Coulomb interaction of Eq. (2.1),

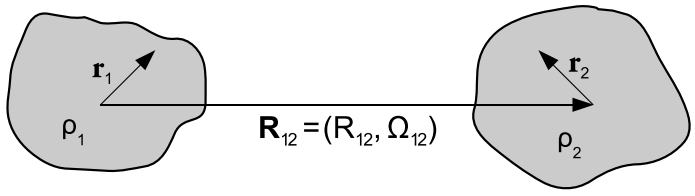

Figure 2.1: Schematic illustration of two interacting charge distributions ρ_1 and ρ_2.

yielding

$$\frac{b_{00}(\Omega_{12})}{R_{12}} = u_{q_1 q_2} = \frac{q_1 q_2}{4\pi\varepsilon_0 R_{12}}, \tag{2.4}$$

where q_i is the net charge or electrostatic *monopole moment* of ρ_i, formally defined as

$$q_i = \int \rho_i(\mathbf{r}_i)\,d\mathbf{r}_i. \tag{2.5}$$

We notice that this term is independent of the orientations of the charge distributions, and thus of Ω_{12}.

For charge distributions having zero net-charge, such as two neutral molecules, the leading-order term is the one with $\ell_1 = \ell_2 = 1$, called the *dipole–dipole* interaction, given by

$$\frac{b_{11}(\Omega_{12})}{R_{12}^3} = u_{\mu_1\mu_2} = \frac{\boldsymbol{\mu}_1 \cdot \boldsymbol{\mu}_2 - 3(\boldsymbol{\mu}_1 \cdot \hat{\mathbf{R}}_{12})(\boldsymbol{\mu}_2 \cdot \hat{\mathbf{R}}_{12})}{4\pi\varepsilon_0 R_{12}^3}, \tag{2.6}$$

where $\hat{\mathbf{R}}_{12}$ is a unit vector pointing in the direction of $\mathbf{R}_{12}$. The Cartesian dipole of ρ_i is, similarly to Eq. (2.5), defined as

$$\boldsymbol{\mu}_i = \int \rho_i(\mathbf{r}_i)\mathbf{r}_i\,d\mathbf{r}_i. \tag{2.7}$$

We note that the dipole–dipole interaction is, unlike the Coulomb interaction, orientation dependent through the scalar products in Eq. (2.6). Furthermore, it decays with separation as R^{-3}, compared to the slower R^{-1} decay of the Coulomb interaction.

The above identification can be continued indefinitely to yield higher terms in the multipole expansion, with increasingly fast separation and orientation dependences. For a given ℓ, the multipole moment is called the "2^ℓ-pole

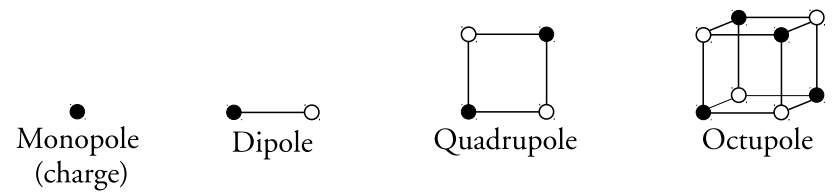

Figure 2.2: Examples of charge distributions corresponding to the four lowest multipole moments, built up from point charges of equal magnitudes and opposite signs, denoted by filled and open circles.

moment"[1] (dipole, quadrupole, octupole, etc.) of ρ. In Figure 2.2, examples of the lowest four multipole moments for the case when ρ is composed of a set of point charges are shown.

The dipole depicted in Figure 2.2, consisting of two point charges $+q$ and $-q$ separated by a vector $\mathbf{d}$, can be thought of as a reasonable model for a diatomic heteronuclear molecule, such as HCl. Using the formal definition from Eq. (2.7) it can be shown that the dipole of this charge distribution equals

$$\boldsymbol{\mu} = q\mathbf{d}. \tag{2.8}$$

For intermolecular separations R much larger than the length d of the dipole, the electrostatic interaction energy between two such dipoles can be shown to reduce to the functional form of Eq. (2.6). Even though all real dipoles have a finite extension, a charge distribution that exactly obeys Eq. (2.6) can be obtained by letting $d = |\mathbf{d}| \to 0$ while letting $q \to \infty$ in such a way that the product $\mu = |\boldsymbol{\mu}| = qd$ remains constant. Such a dipole is called an *ideal* or *point* dipole. An ideal dipole is usually depicted as a vector pointing from the negative to the positive charge, which is also the convention we will adopt here.

2.2 Angle-averaged interactions

In the previous section, we considered the electrostatic interaction between two stationary charge distributions, such as two dipolar molecules having fixed orientations. In a real gas or liquid, however, the molecules are constantly moving randomly due to the thermal motion present at nonzero temperatures. The purpose of this section is to show how the interaction $u_{\mu_1\mu_2}$ of Eq. (2.6) between two dipoles having fixed orientations is altered when the dipoles are allowed to rotate due to thermal motion.

According to basic statistical thermodynamics (see further Chapter 3), the averaged ("effective") interaction $w_{\mu_1\mu_2}(R_{12})$ between two rotating dipoles can be obtained by weighting each configuration with its Boltzmann factor e^{-u/k_BT} and integrating over the orientational degrees of freedom. Ignoring normalization factors, this integral thus becomes

$$w_{\mu_1\mu_2}(R_{12}) \propto \int u_{\mu_1\mu_2}(R_{12}, \Omega_{12}) e^{-u_{\mu_1\mu_2}(R_{12},\Omega_{12})/k_BT} d\Omega_{12}, \tag{2.9}$$

[1] Formally, the term "2^ℓ-pole moment" is used to denote the *magnitude* of the quantity, whereas for the tensor quantity (having both magnitude and direction) the word "moment" is dropped. In practice, however, "2^ℓ-pole moment" is often used to denote both the scalar and tensor quantities.

where k_B is Boltzmann's constant and T is the temperature. Even though this integral is not analytically solvable, we may expand the Boltzmann factor to leading order, which is a good approximation when $u_{\mu_1\mu_2}(R_{12}, \Omega_{12}) < k_B T$, i.e. for large separations, small dipole moments, and/or high temperatures. The final approximate result for $w_{\mu_1\mu_2}(R_{12})$ is

$$w_{\mu_1\mu_2}(R_{12}) \approx -\frac{2\mu_1^2\mu_2^2}{3(4\pi\varepsilon_0)^2 k_B T R_{12}^6}. \tag{2.10}$$

Clearly, this potential has a considerably faster decay with separation (R_{12}^{-6} rather than R_{12}^{-3}) compared to the unweighted one, and is always attractive, due to the Boltzmann factor favoring configurations with attractive values of $u_{\mu_1\mu_2}$.

The interaction between two freely rotating dipoles is sometimes called the *Keesom interaction*, and constitutes one of the three R_{12}^{-6} contributions to the so-called van der Waals interaction, the others being the permanent dipole–induced dipole ("Debye") and induced dipole–induced dipole ("London") interactions. The Keesom term is also the only one of these three interaction mechanisms that can be described entirely using classical electrostatics.

Most experimentally relevant systems requires a description of van der Waals interactions between bodies composed of many interacting molecules. Since angle-averaged interactions like that of Eq. (2.10) are not pairwise additive, the question of how to calculate the separation-dependent interaction free energy between two bodies composed of dipoles is difficult even for idealized geometries such as planes, spheres and cylinders [18]. It is, however, handled in an accurate way by the classical Lifshitz theory of van der Waals interactions [19] as well as in approximate ways by simpler theories. In Papers IV and V, we will use an alternative formalism to describe the interaction

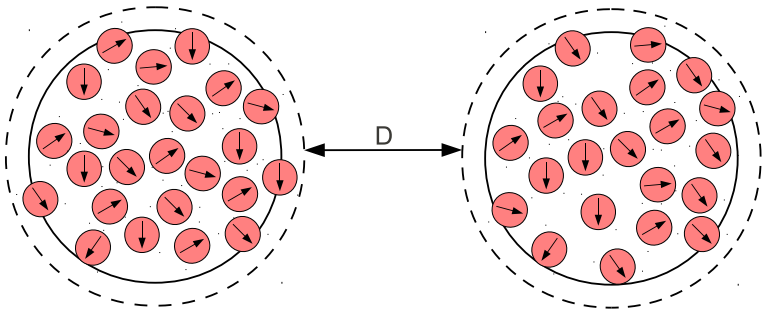

Figure 2.3: Schematic illustration of two interacting colloidal particles composed of permanent dipoles, separated by a distance D.

between two spherical bodies of dipoles (see Figure 2.3) as a function of their separation D.

2.3 Dielectric continuum theory

We now consider the case of a plane-plate capacitor depicted in Figure 2.4, composed of two conducting plates carrying opposite surface charges $+\sigma$ and $-\sigma$, separated either by vacuum or by a non-conducting medium. In the case when there is vacuum between the plates, the difference in electrostatic potential due to the surface charges on the respective plates will induce a constant electrostatic field of magnitude $E_{vac} = \sigma/\varepsilon_0$ in the slit. However, when a polar medium is present between the plates, the dipoles will on average orient themselves in the applied field, effectively counteracting, or *screening*, it. The ability of a fluid to screen electric fields depends on several parameters, such as its density, the size of its dipole moment, and its molecular polarizability. In spite of this rather complicated physical situation, the screening ability of a fluid can be characterized through the *relative dielectric permittivity* or *dielectric constant* ε_r, which gives the magnitude of the electric field inside the capacitor relative to the value it would have in the absence of any medium between the plates:

$$E_{medium} = E_{vac}/\varepsilon_r = \sigma/\varepsilon_0\varepsilon_r. \tag{2.11}$$

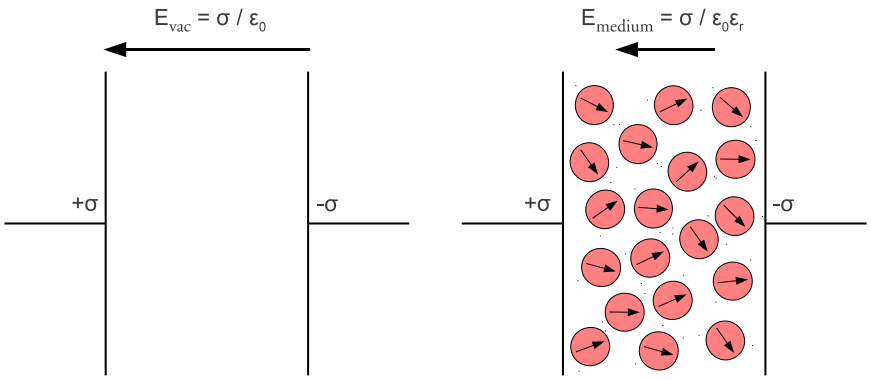

Figure 2.4: A plane-plate capacitor without (left) and with (right) a dipolar fluid between the plates. The dipoles orient themselves according to the sign of the applied surface charges $+\sigma$ and $-\sigma$, effectively diminishing the field by a factor ε_r.

Since the interaction between charged objects is mediated by electric fields, the presence of a medium between the objects will alter the interaction potential of Eq. (2.1) by a factor ε_r:

$$u_{q_1 q_2}^{(\mathrm{med})} = \frac{u_{q_1 q_2}^{(\mathrm{vac})}}{\varepsilon_r} = \frac{q_1 q_2}{4\pi\varepsilon_0 \varepsilon_r r_{12}}. \tag{2.12}$$

Thus, two ions in a high-dielectric medium experience a significantly weaker interaction than two ions in free space. This phenomenon can be used to explain, among many other phenomena, the high solubility of ions in water ($\varepsilon_r \approx 80$) compared to that in oil ($\varepsilon_r \approx 2$).

The dielectric approximation is equivalent to removing all the molecular details of the solvent, and replacing it with a uniform, structureless dipolar density implicitly contained in ε_r. Even though the simplification involved in replacing a large number of molecules by a just a single number is tremendous, the dielectric continuum model has shown successful to qualitatively describe many central phenomena in colloidal science. One of its most impressive applications is the so-called *primitive model* of electrolytes, where aqueous salt solutions are modeled by simply removing the water molecules and at the same time replacing the Coulombic interaction potential [Eq. (2.1)] between the ions, modeled as charged hard spheres, by its screened counterpart [Eq. (2.12)].

An appealing property of dielectric continuum models is that the associated problems can usually be solved analytically using only standard relations from classical electrostatics, whereas molecular models are often very difficult, if not impossible, to solve without the help of computer simulation techniques.

2.4 Electrostatic fluctuations

Even though the models that will be considered in this thesis describe fluids whose particles possess only a dipole moment, a *collection* of such particles in general also possesses multipole moments of all orders higher than the dipole. For example, the spherical bodies of dipolar particles depicted in Figure 2.3 each possess a nonzero dipole, quadrupole, octupole, etc., relative to an arbitrary origin. Because of thermal fluctuations, each of these multipole moments will fluctuate around its equilibrium value. In an isotropic system such as a spherical sub-volume inside a fluid of infinite extent the mean value is zero, since each multipole component (for example the three Cartesian dipole components) will take on positive and negative values with equal probabilities.

Using the dielectric continuum description introduced in the previous section, we may relate the magnitude of the fluctuations of each multipole moment to the dielectric constant of the medium. It is shown in Paper I that the fluctuating axial 2^ℓ-pole moment M_ℓ of a sphere of dielectric material surrounded by vacuum (see Figure 2.5) can be described by a Gaussian probability distribution $P(M_\ell)$, i.e.

$$P(M_\ell) \propto e^{-\alpha M_\ell^2}, \tag{2.13}$$

where the positive exponent α is related to ε_r and the radius R of the sphere through

$$\alpha = \frac{[\ell(\varepsilon+1)+1]}{2\ell(\varepsilon-1)k_B T}\frac{1}{R^{2\ell+1}}. \tag{2.14}$$

Note that we have dropped the "r" subscript on ε, and that we are now using reduced units where $4\pi\varepsilon_0 = 1$. When the sphere of dielectric material is brought from vacuum ($\varepsilon_{sur} = 1$) into an infinite volume of its own medium ($\varepsilon_{sur} = \varepsilon$), the surrounding medium will create a reaction field on the sphere, thus making it easier to create large values of M_ℓ. Thus, $P(M_\ell)$ will become wider, corresponding to larger fluctuations. However, it is still described by a Gaussian function, whose exponent $\widetilde{\alpha}$ is now given by

$$\widetilde{\alpha} = \frac{(2\ell+1)^2\varepsilon}{2(\varepsilon-1)\ell\,[(\ell+1)\varepsilon+\ell]\,k_B T}\frac{1}{R^{2\ell+1}}. \tag{2.15}$$

A plot of $P(M_2)$ (i.e., the axial quadrupole moment) for a dielectric sphere with $\varepsilon = 80$ in vacuum and immersed in its own medium is shown in Figure 2.6.

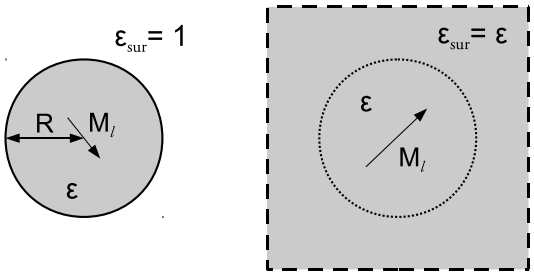

Figure 2.5: Schematic illustration of the fluctuating axial 2^ℓ-pole moment M_ℓ of a dielectric sphere in a vacuum (left) and immersed in its own medium (right).

The concept of probability distributions describing the fluctuating multipole moments in a polar fluid, described either as a dielectric continuum or as a fluid of discrete particles, forms the basis for all the studies included in this thesis. By using concepts from basic statistical thermodynamics, we will show how these probability distributions [i.e., Eqs. (2.13) – (2.15)] can be used to describe solvation energies and van der Waals interactions, as well as assessing the accuracy of different computer simulation techniques.

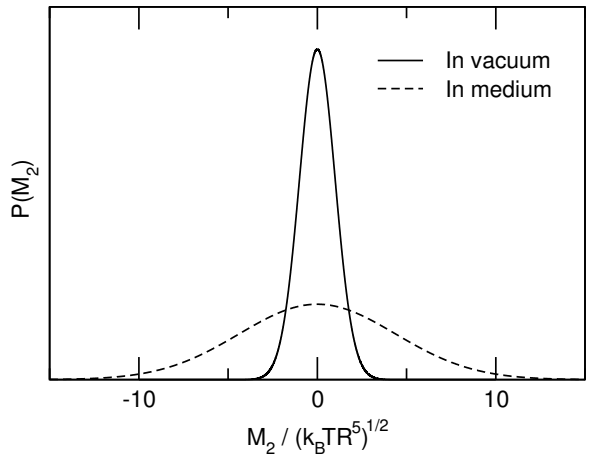

Figure 2.6: Probability distribution $P(M_2)$ of the axial quadrupole moment M_2 (in reduced units) of a dielectric sphere with $\varepsilon = 80$ obtained from Eqs. (2.13), (2.14), and (2.15).

CHAPTER
THREE

STATISTICAL THERMODYNAMICS

The field of statistical thermodynamics (or, alternatively, statistical mechanics) provides a theoretical framework that relates the microscopic details of a system to its macroscopic thermodynamic properties. For example, given molecules with certain known properties (size, polarizability, geometry, etc.), statistical thermodynamics can inform us, at least in principle, about how a material made up of the same molecules will behave on the macroscopic scale, through for example its phase behavior or solubility. Most of the concepts of this chapter are elaborated in the books by Hill [20] and McQuarrie [21] as well as in several other textbooks on the subject.

3.1 Entropy from a molecular viewpoint

Arguably, the most fundamental equation of statistical thermodynamics, first stated by Ludwig Boltzmann (1844–1906) in the late 19$^{\text{th}}$ century, is the statistical definition of the entropy S of an isolated system:

$$S = k_B \ln \Omega(N, V, U), \tag{3.1}$$

where $k_B \approx 1.38{\cdot}10^{-23}$ J/K again denotes Boltzmann's constant and $\Omega(N, V, U)$ is the number of possible configurations of the system that are compatible with a given constant number of particles N, system volume V and total (kinetic and potential) energy U. If the system consists of a fluid composed of discrete particles, a configuration is the set of simultaneous positions and momenta of all particles; in total a $6N$-dimensional function. Thus, Eq. (3.1) is compatible with the common description of high-entropic systems as being disordered, i.e. having many possible configurations, and low-entropic ones

being ordered, with few accessible configurations. Together with the second law of thermodynamics [22], stating that nature always strives to increase the entropy of an isolated system, it can even be used as a way to define the direction of the arrow of time, i.e. to distinguish the past from the present.

The beauty of Eq. (3.1) lies in that it gives a microscopic interpretation (particle positions and momenta) of a macroscopic property (the entropy) which is not provided by classical thermodynamics; indeed, classical thermodynamics treats entropy as a somewhat *ad hoc* function having certain properties, without providing any further interpretation of it. Given that the very existence of atoms and molecules was a controversial issue when Boltzmann made his microscopic interpretation of thermodynamics, his work was not fully appreciated until long after his death. In fact, it was not until the advent of reasonably fast electronic computers about 70 years later that the full potential of his methods could be exploited.

3.2 Central relations in the canonical ensemble

The entropy definition of Eq. (3.1) is valid for an isolated system, in other words a system that cannot exchange energy or particles with its surroundings. In statistical thermodynamic language, the set of possible configurations of such a system, all having the same value of N, V, and U, constitutes the *microcanonical ensemble*. For many physical and chemical applications, however, it is often more relevant to consider a system which is thermally connected to the surrounding environment, meaning that the energy of the system is no longer kept constant. This corresponding set of configurations having the same values of N, V, and T, weighted by their respective probabilities, is denoted the *canonical* ensemble.

In an analogous way, one may let the system exchange particles with its surroundings by fixing the chemical potential μ, yielding the *grand canonical* (constant μ, V, and T) ensemble, or to allow for changes in volume of the system by working in the *isothermal–isobaric* (constant N, P, and T, where P is the pressure) ensemble. Which ensemble one chooses to work in depends largely on the problem one seeks to solve, and is a matter of convenience rather than of physical correctness. In fact, in the thermodynamic limit (i.e., for infinitely large systems), the results of a calculation are independent of the chosen ensemble, even though there can be orders of magnitude of difference between the complexities of the analyses. Throughout the studies contained in this thesis we will work within the canonical ensemble, in the context of which we will now discuss some central relations.

As stated in the previous section, the second law of thermodynamics

states that any isolated system has its equilibrium position where its entropy is at a maximum. For a constant N, V, T system that can exchange energy with its surroundings, however, the relevant property to consider is the Helmholtz free energy A, defined by

$$A = -k_B T \ln Q(N, V, T). \tag{3.2}$$

$Q(N, V, T)$ is called the *canonical partition function*, defined according to

$$Q(N, V, T) = \sum_U \Omega(N, V, U) e^{-\beta U}, \tag{3.3}$$

where the sum runs over all possible energies of the system, and we have used the standard abbreviation $\beta = (k_B T)^{-1}$. Due to the minus sign in the definition of A, the Helmholtz free energy is always at a minimum for a closed equilibrium system thermally coupled to its surroundings. The effect of the exponential factor in Eq. (3.3) is to weight each configuration depending on its energy, in the sense that low energy configurations occur more often than those having a high energy. In fact, it can be shown that the probability P_i of observing a configuration i having an energy U_i is proportional to this so-called Boltzmann factor, i.e.

$$P_i(U_i) \propto e^{-\beta U_i}, \tag{3.4}$$

which is also the relationship we used when deriving Eq. (2.10).

The summation sign in Eq. (3.3) assumes that the configurations of the system are discrete and countable, which is the case for systems where quantum effects are significant. This is, however, not a convenient description for systems of particles obeying classical mechanics, where the energy is an essentially continuous function of the positions and momenta of the particles. Thus, when treating fluids consisting of classical particles, such as the model systems used throughout this thesis, it is preferable to change the sum in Eq. (3.3) for an integral and express the classical partition function $Q_{\text{class}}(N, V, T)$ as

$$Q_{\text{class}}(N, V, T) = \frac{1}{N! h^{3N}} \iint e^{-\beta U(\mathbf{r}^N, \mathbf{p}^N)} d\mathbf{r}^N d\mathbf{p}^N, \tag{3.5}$$

where h is Planck's constant and the integral runs over all positions $\mathbf{r}^N$ and momenta $\mathbf{p}^N$ of the N particles. Furthermore, for a system obeying classical mechanics, it is always possible to separate the kinetic part, depending on $\mathbf{p}^N$, from the configurational part, that depends only on $\mathbf{r}^N$, in the partition function. By inserting the expression

$$\mathcal{U}_{\text{kin}}(\mathbf{p}^N) = \sum_{i=1}^{N} \frac{p_i^2}{2m} \tag{3.6}$$

for the kinetic energy $\mathcal{U}_{\text{kin}}(\mathbf{p}^N)$, where m is the particle mass, into Eq. (3.5) and performing the integral over momenta, one arrives at

$$Q_{\text{class}}(N,V,T) = \frac{1}{\Lambda^{3N}N!}\int e^{-\beta\mathcal{U}_{\text{pot}}(\mathbf{r}^N)}\,d\mathbf{r}^N \equiv \frac{Z}{\Lambda^{3N}N!}, \tag{3.7}$$

where $\mathcal{U}_{\text{pot}}(\mathbf{r}^N)$ is the potential energy of the system, and $\Lambda = h/\sqrt{2\pi m k_B T}$ is called the de Broglie wavelength. This prefactor can be precalculated easily, meaning that the essential information of the classical partition function is contained in the *configuration integral*, Z, defined by Eq. (3.7). The configuration integral is a central property in the sense that it contains information about all equilibrium properties of a classical system. Unfortunately, this also means that it is usually very difficult to obtain it exactly, apart from when working with very simple model systems. The fact that Z only depends on the particle positions leads us to the rather remarkable conclusion that the equilibrium properties of any classical system are independent of the system dynamics.

Using Eqs. (3.2) and (3.7), we find that the change $\Delta A_{1\to 2}$ in Helmholtz free energy when going from one thermodynamic state to another is simply given by the ratio of their configuration integrals:

$$\Delta A_{1\to 2} = -k_B T \ln \frac{Z_2}{Z_1}, \tag{3.8}$$

where we have used the fact that Λ and N are kept constant. Furthermore, using Eq. (3.4) together with some statistical considerations, one can derive an expression for the thermal average $\langle \mathcal{B} \rangle$ of some quantity $\mathcal{B}(\mathbf{r}^N)$ that may represent, for example, the system energy, pressure, or chemical potential:

$$\langle \mathcal{B} \rangle = \frac{\int \mathcal{B}(\mathbf{r}^N) e^{-\beta\mathcal{U}_{\text{pot}}(\mathbf{r}^N)}\,d\mathbf{r}^N}{\int e^{-\beta\mathcal{U}_{\text{pot}}(\mathbf{r}^N)}\,d\mathbf{r}^N}. \tag{3.9}$$

Equations (3.8) and (3.9) give access to a large amount of thermodynamic information for systems where $\mathcal{U}_{\text{pot}}(\mathbf{r}^N)$ is known. In the next section, a few examples will be given of actual model systems to which these relations can be applied.

3.3 Model systems and interaction potentials

In the previous section, we used the term "system" in a rather general way, without going into details about how the potential energy $\mathcal{U}_{\text{pot}}(\mathbf{r}^N)$ of the system might look like. The process of choosing a functional form for the

potential energy is equivalent to choosing a model system that contains the basic properties relevant for the physical problem one wants to study. Of course, the degree of complexity of such models may vary tremendously. In this section we will merely exemplify using some relatively simple fluid models that bear relevance for the studies contained in the thesis.

The simplest possible model of a fluid is that of a gas of non-interacting particles, an *ideal gas*, for which $\mathcal{U}_{\text{pot}}(\mathbf{r}^N) = 0$. This is one of the few systems for which the configuration integral can be easily calculated, simply yielding $Z = V^N$. The ideal gas is a very useful model for describing dilute gases, but naturally fails to predict properties of denser gases and liquids.

A more realistic model of simple monatomic fluids, such as the noble gases, is the Lennard-Jones potential, which has the functional form

$$u_{LJ}(r_{ij}) = 4\varepsilon \left[\left(\frac{\sigma}{r_{ij}} \right)^{12} - \left(\frac{\sigma}{r_{ij}} \right)^{6} \right], \tag{3.10}$$

where r_{ij} is the separation between particles i and j, and ε and σ are parameters that determine the strength of the interaction and the particle size, respectively. In Figure 3.1, the functional form of the Lennard-Jones potential is shown. The attractive r^{-6} term is meant to mimic the dispersion interaction between atoms, whereas the repulsive r^{-12} term in an *ad hoc* way models the short-range Pauli repulsion. The total energy $\mathcal{U}_{LJ}(\mathbf{r}^N)$ is then obtained by assuming that the interparticle interactions are pairwise additive, i.e.

$$\mathcal{U}_{LJ}(\mathbf{r}^N) = \sum_{i=1}^{N-1} \sum_{j=i+1}^{N} u_{LJ}(r_{ij}). \tag{3.11}$$

Although the assumption of pairwise additivity is not strictly correct for dispersion interactions, the Lennard-Jones model is still capable of reproducing several features of, for example, liquid argon. Unfortunately, even this seemingly simple interaction potential is complex enough to make it impossible to solve the corresponding configuration integral exactly. However, several approximate analytical approaches as well as computer simulation techniques have been used to determine the thermodynamic properties of Lennard-Jones fluids [23].

One of the most widely investigated models of polar fluids, which will also be thoroughly explored in this thesis, is the so-called Stockmayer fluid, originally introduced by Walter Stockmayer (1914–2004) in 1941 for the study of polar gases. This model combines the Lennard-Jones potential of Eq. (3.10) with the point-dipole interaction of Eq. (2.6), yielding

$$u_{SM}(r_{ij}, \omega_i, \omega_j) = u_{LJ}(r_{ij}) + u_{\mu_i \mu_j}(r_{ij}, \omega_i, \omega_j), \tag{3.12}$$

where ω_i and ω_j denotes the orientations of particles i and j. The Stockmayer potential is also summed up in a pairwise fashion as in Eq. (3.11). Since the pairwise additivity holds exactly for the dipolar part of the interaction, as for all electrostatic interactions, the pairwise summation does not constitute any further approximation. The anisotropy of the Stockmayer potential, introduced through the angular dependence of the dipole–dipole interaction, together with its long range makes it a significantly more complex model to investigate than the Lennard-Jones fluid. In this thesis, computer simulation methods will be used to investigate different electrostatic properties of the Stockmayer fluid. Thus, the emphasis will lie heavily on the dipolar part of the interaction, whereas the Lennard-Jones interaction is merely included to increase the physical realism of the model.

All the models described above involve discrete particles, and the potential energy $\mathcal{U}_{\text{pot}}$ is thus a function of all the positional coordinates $\mathbf{r}^N$ and, in the case of Stockmayer particles, all the orientations $\boldsymbol{\omega}^N$ of the particles. The statistical-mechanical framework can, however, also be used to treat the dielectric continuum model described in Section 2.4. Formally, this means that the set of positions and orientations of all particles are exchanged for the set of electric multipole moments as the relevant parameters determining the potential energy, i.e.

$$\mathcal{U}_{\text{pot}}(\mathbf{r}^N, \boldsymbol{\omega}^N) \rightarrow \mathcal{U}_{\text{pot}}(M_\ell). \tag{3.13}$$

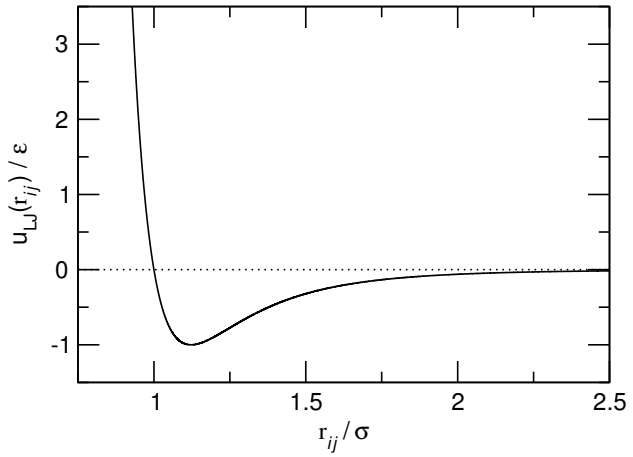

Figure 3.1: Plot showing the Lennard-Jones potential, obtained from Eq. (3.10). The minimum occurs at $r_{ij} = 2^{1/6}\sigma$, and takes the value $u_{LJ} = -\varepsilon$.

As an example system, we will use the thermally fluctuating dielectric sphere discussed in Section 2.4, for which we obtained exact expressions for the probability distributions $P(M_\ell)$. By comparing Eq. (3.4) with Eqs. (2.13), (2.14), and (2.15) we can identify an expression for the energy $\mathcal{U}(M_\ell)$ connected with the creation of an instantaneous multipole moment M_ℓ in vacuum and in a medium, which can then be used to evaluate the corresponding configuration integrals. In paper II, we use these considerations together with Eq. (3.8) to calculate the change in Helmholtz free energy $\Delta A_{\text{vac}\to\text{med}}$ for bringing a sphere of dielectric material from vacuum into a surrounding medium (Figure 2.5). The solvation free energy connected to the solvation of the axial 2^ℓ-pole moment is thus found to be

$$\Delta A_{\text{vac}\to\text{med}} = -k_B T \ln \frac{Z_{\text{med}}}{Z_{\text{vac}}} = -k_B T \ln \frac{\alpha}{\widetilde{\alpha}}, \tag{3.14}$$

which can be evaluated exactly by inserting Eqs. (2.14) and (2.15) for the exponents α and $\widetilde{\alpha}$, respectively. The rather remarkable fact that we are able to exactly solve the configuration integrals for the dielectric continuum model, in spite of the very complex nature of the dipole–dipole interaction it models, highlights the significance of such simplified models in gaining a physical understanding of complex systems like dipolar fluids.

CHAPTER

FOUR

COMPUTER SIMULATIONS

The term "computer simulations" encloses a plethora of numerical methods used to obtain thermodynamic information about physical models such as those discussed in Section 3.3. In this chapter we will cover the two most popular methods, namely Monte Carlo (MC) and molecular dynamics (MD) simulations, together with some of the technical issues encountered when dealing with the simulation of molecular systems. For a more thorough introduction to the subject of computer simulation techniques, the books by Frenkel and Smit [12] and Allen and Tildesley [24] are recommended.

Throughout this chapter, we will for simplicity assume that the particles are isotropic, meaning that the interaction potential $u(r_{ij})$ only depends on the intermolecular separation r_{ij}, and furthermore that the intermolecular potential is pairwise additive.

4.1 Monte Carlo simulations

As was discussed in the previous chapter, the way to determine thermodynamic averages in the canonical ensemble is by solving the integrals in Eq. (3.9), which may not seem as such a daunting task as long as the analytic form of the interaction potential $\mathcal{U}_{pot}(\mathbf{r}^N)$ is known. A straightforward way of solving integrals like this would be to just randomly create particle configurations, calculate $\mathcal{U}_{pot}(\mathbf{r}^N)$ and $\mathcal{B}(\mathbf{r}^N)$, and sample the integrands of Eq. (3.9) for each configuration, thus constructing a 3N-dimensional functional surface that can be integrated numerically. However, for all but very dilute systems, most such random configurations will have large particle overlaps, yielding strongly repulsive interactions (i.e., $\mathcal{U}_{pot} \gg k_BT$). Thus, the Boltz-

mann factors present in both integrands of Eq. (3.9) will be very small, and the contribution to the integral from such configurations will be completely negligible. This way of sampling configuration space thus turns out to be extremely inefficient, since most of the computational time is spent on sampling essentially zero-valued functions.

A very elegant solution to this problem was presented through the so-called Metropolis algorithm [25] which, in spite of its name, was developed by the Rosenbluth and Teller couples at the Los Alamos laboratory in conjunction with the US nuclear program in the 1950's [26]. The basic idea behind the algorithm is that instead of performing a uniform sampling of configuration space followed by a weighted averaging, one creates configurations with a probability proportional to the Boltzmann factor followed by an *unweighted* averaging procedure. In other words, the algorithm steers the system towards configurations having a high probability, thus avoiding the sampling of uninteresting parts of configuration space. A basic implementation of the Metropolis algorithm goes as follows:

1. Generate a random configuration.

2. Select one particle in the system and displace it a random distance in space.

3. Calculate the difference $\Delta\mathcal{U}_{\text{pot}}$ in potential energy between the new and the old configuration.

4. If the energy of the new configuration is lower than that of the old configuration ($\Delta\mathcal{U}_{\text{pot}} < 0$), store the new configuration. If the energy has increased ($\Delta\mathcal{U}_{\text{pot}} > 0$), store the new configuration with a probability $e^{-\beta\Delta\mathcal{U}_{\text{pot}}}$ by comparing with a random number; otherwise, restore the old one.

5. Sample the thermodynamic data of interest from the stored configuration. Note that when the new configuration is rejected, this means a resampling from the old configuration. The values sampled from the initial part of the simulation, before the system has reached equilibrium, are, however, to be discarded.

6. Repeat from point 2.

The central concept of this procedure is point 4 above, which ensures that configurations are generated with probabilities proportional to their Boltzmann factors. This "importance sampling" leads to a tremendous increase in

the sampling efficiency, compared to an unbiased sampling of configuration space. It, however, comes at the price of not being able to explicitly calculate the configuration integral, which means that the free energy A is not directly accessible without using more elaborate techniques such as thermodynamic integration [12], which requires performing simulations at several different temperatures. We also note that the temperature is treated as a constant parameter in point 4 above. Thus, the proper ensembles to use for a Metropolis MC simulation are those where the temperature is kept constant, with the canonical (constant N, V, T) ensemble being the natural choice for most physical problems.

The numerical robustness of the Metropolis algorithm enables the use of almost any type of "trial move" during the course of the simulation, in addition to the simple lateral displacement of a single particle used in point 2 of the above example. The only constraint put on a trial move is that it leads to a sampling of configuration space consistent with the particular ensemble being used. These alternative trial moves include, for example, rotations and displacements of whole groups of particles ("cluster moves") or chain segments ("pivot rotations") when simulating polymeric systems. It may also include rescaling the size of the whole system when working in the isothermal–isobaric ensemble or the insertion/deletion of particles from the system in the grand canonical ensemble.

4.2 Molecular dynamics simulations

A conceptually very different, but perhaps more straightforward, way of studying a molecular model system in a computer is to simply let the molecules interact and move according to Newton's laws of classical mechanics, in particular the one which relates the force $\mathbf{F}$ acting on a body to its acceleration $\mathbf{a}$:

$$\mathbf{F} = m\mathbf{a}. \tag{4.1}$$

For systems where the intermolecular potential $u(r_{ij})$ is known analytically, such as a Lennard-Jones fluid, the force $\mathbf{F}_i$ acting on particle i can be obtained in a straightforward manner by differentiating the potential and summing the force contributions coming from all other particles:

$$\mathbf{F}_i = -\sum_{j \neq i} \nabla u(r_{ij}). \tag{4.2}$$

The time evolution of the system can then be studied by making a Taylor expansion relating the position $\mathbf{r}_i(t)$ of particle i at time t to the position of

the same particle a short time Δt later:

$$\mathbf{r}_i(t + \Delta t) = \mathbf{r}_i(t) + \boldsymbol{v}_i(t)\Delta t + \frac{\boldsymbol{a}_i(t)}{2}\Delta t^2 + \ldots, \tag{4.3}$$

where $\boldsymbol{v}_i$ denotes the velocity of particle i. By writing down the corresponding expansion for $\mathbf{r}_i(t - \Delta t)$ and summing up the expressions to third order now yields the so-called Verlet algorithm [27], according to

$$\mathbf{r}_i(t + \Delta t) = 2\mathbf{r}_i(t) - \mathbf{r}_i(t - \Delta t) + \boldsymbol{a}_i(t)\Delta t^2 + \mathcal{O}(\Delta t^4). \tag{4.4}$$

Thus, to evolve the system one time step one needs to have access to the particle positions two time steps back, and the particle accelerations [obtained through Eqs. (4.1) and (4.2)] one time step back. In spite of its simplicity, the Verlet algorithm is very robust, and thus one of the most popular MD integrators, even though other useful alternatives exist [12].

An obvious advantage of using MD simulations is that they, unlike Monte Carlo-based techniques, give access to dynamic information about the system, and can thus also be used to study non-equilibrium processes such as the dynamics of self-assembly and protein folding. On the other hand, MD methods are limited by the fact that the system must evolve according to Newtonian mechanics, whereas the different moves in an MC simulation are allowed to violate Newton's laws. This also means that "hard" potentials, that vary very steeply or even discontinuously with separation, are not easily handled in MD simulations.

For sufficiently small values of Δt, the Verlet algorithm (and any other good integrator) conserves the total energy U of the system. Thus, the natural ensemble for running an MD simulation is the microcanonical ensemble. Since it is usually preferable to work in an ensemble where temperature rather than energy is conserved, several methods ("thermostats") exist that couple the simulation to an external heat bath of constant temperature. Two of these, named after Andersen [28] and Nosé–Hoover [29, 30], have been shown to formally yield a true canonical distribution, whereas the so-called Berendsen thermostat [31] used throughout this work merely weakly suppresses the fluctuations in kinetic energy, and thus in temperature, of the system. Similarly, there are algorithms ("barostats") that introduces volume fluctuations into the system, making it possible to run MD simulations in the isothermal–isobaric ensemble [12].

In the end, it is often merely a matter of personal preference whether one chooses to follow the MC or the MD path to solving the properties of a particular model system. For the studies included in this thesis, we will use both methods to obtain thermodynamic data of Stockmayer fluids.

4.3 Handling interactions

Even though modern computers make it possible to simulate systems containing about a million particles, this is still far from the number of molecules ($N \approx 10^{20}$) contained in a typical bulk system. This is a significant problem if one wants to simulate bulk properties of a fluid. As an example, in a spherical container containing 10^6 water molecules, about 15% of the molecules will still reside within a nanometer from the surface, and the influence from the bounding surface on the system properties will thus be significant.

The standard way of handling this problem is the use of *toroidal boundary conditions* (usually called *periodic* boundary conditions; see footnote on page 31). Put simply, these are imposed by letting any particle that passes through the imaginary boundary of the simulation cell reenter the cell through the opposite side, as depicted in two dimensions in Figure 4.1. Topologically, this means that the boundaries of the three-dimensional space are connected to yield a toroidal body in four dimensions, very much like connecting the ends of a one-dimensional rope to yield a two-dimensional circle.

In addition to toroidal boundary conditions, we also need a way to calculate the potential energy of the system. The most straightforward way of doing this is to use the approach already discussed in Section 3.3, namely to consider the interaction between all N particles inside the simulation cell, according to

$$\mathcal{U}_{\text{pot}}(\mathbf{r}^N) = \sum_{i=1}^{N-1} \sum_{j=i+1}^{N} u(r_{ij}). \tag{4.5}$$

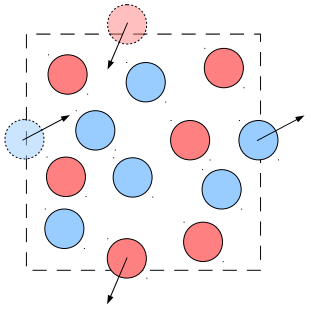

Figure 4.1: Schematic illustration of toroidal boundary conditions in two dimensions. As the particles marked by arrows exit through the imaginary boundary, they reenter the simulation cell from the opposite side, thus eliminating the physical boundary from the system.

This so-called *minimum image convention* in practice leads to a cubic cut-off of the potential. Alternatively, one may exclude the particles residing in the corners of the simulation cell by instead using a spherical cut-off:

$$\mathcal{U}_{pot}(\mathbf{r}^N) = \sum_{i=1}^{N-1} \sum_{j=i+1}^{N} u(r_{ij})\Theta(r_{cut} - r_{ij}). \tag{4.6}$$

In Eq. (4.6), the Heaviside function $\Theta(r_{cut} - r_{ij})$ goes from 1 to 0 when $r_{ij} > r_{cut}$, thus excluding the interaction between particles having a separation larger than the cutoff radius r_{cut}.

However, the cut-off schemes above make it impossible to consider the interaction between particles further away from each other than the physical dimensions of the simulation cell, which is usually a small distance compared to in a true bulk system. To estimate the magnitude of this finite-size effect, we assume that the fluid has a uniform particle density ρ beyond the cut-off radius, and estimate the long-range interaction u_{LR} between a central particle and all the particles *beyond* the cut-off sphere:

$$u_{LR} = \int_{r_{cut}}^{\infty} u(r) 4\pi r^2 \rho dr, \tag{4.7}$$

where $4\pi r^2 \rho dr$ is the number of particles located in a spherical shell of thickness dr located at a distance r from the central particle. We now consider the particular case when $u(r)$ has an inverse power-law form, i.e. $u(r) = Cr^{-n}$ with some arbitrary constant C and positive exponent n. This general form encompasses most commonly used intermolecular potentials, and in particular all the models discussed in this thesis. Inserting this expression for $u(r)$ into Eq. (4.7) and solving the integral yields

$$u_{LR} = \begin{cases} 4\pi\rho C \left[(n-3) r_{cut}^{n-3}\right]^{-1} & \text{if } n < 3 \\ \pm\infty & \text{if } n \leqslant 3 \end{cases} \tag{4.8}$$

Thus, for short-range potentials, such as the Lennard-Jones potential ($n = 6$), the long-range part of the interaction decays quickly with increasing cut-off radius. What is more striking, however, is that the long-range parts of the Coulomb ($n = 1$) and dipole–dipole ($n = 3$) interactions are *infinite* for all finite values of r_{cut}. For this reason, one often makes a formal distinction between short-range potentials, decaying faster than r^{-3}, and long-range or infinite range potentials, that decay as r^{-3} or slower.

The infinite range of the electrostatic potentials is indeed a disturbing problem, since it means that one in principle has to simulate a system containing infinitely many particles to obtain realistic values of the thermodynamic

properties. Although this may seem as an impossible task, several solutions to this problem have been proposed through the years. In the following, we will briefly explain the rationale behind the most popular ones.

Cutoff-based methods

The computationally most appealing way to "solve" the long-range interaction problem is to simply ignore it and apply a cubic or spherical cutoff to the electrostatic interactions. Although this has been shown to work for certain problems, in particular for weakly charged and/or dipolar systems, it often leads to serious artifacts [10, 32]. However, simulation schemes have been proposed that screen the long-range potential in order to render it short-range, which again makes it possible to truncate it using a simple spherical cut-off. Even though this approach may seem unphysical, the use of screened potentials for the simulation of Coulombic systems has been shown to give results in good agreement with those obtained using more elaborate techniques [33, 34].

Periodic boundary conditions

Arguably, the most popular set of methods that actually respect the long-range nature of electrostatic interactions are those employing *periodic boundary conditions* (PBCs).[2] Within these methods, the central simulation cell is duplicated in all directions in a space-filling manner. Thus, each particle in the system interacts with all particles in the primary cell, as well as with an infinite array of periodic replicas of itself and all other particles as depicted in Figure 4.2. Mathematically, this leads to a potential energy of the form

$$\mathcal{U}_{\mathrm{PBC}}(\mathbf{r}^N) = \frac{1}{2}{\sum_{\mathbf{n}}}' \left[\sum_{i=1}^{N} \sum_{j=1}^{N} u(r_{ij} + n) \right], \tag{4.9}$$

where $\mathbf{n}$ runs over all points in the lattice of simulation cells, and the prime indicates that the infinite self-interaction terms (i.e., the terms for which $i = j$ and $\mathbf{n} = 0$) should be excluded from the sum.

[2] In the literature, the term "periodic boundary conditions" is often used to denote what we here call *toroidal* boundary conditions, in spite of these not being properly periodic in the crystallographic sense. The use of a truly infinite system (periodic boundary conditions in our terminology) is therefore sometimes called *truly* periodic boundary conditions. More often, however, the name of a specific algorithm (Ewald summation, particle mesh Ewald etc.) is used to denote the use of an infinite periodic system to treat long-range interactions.

Traditionally, periodic boundary conditions have been implemented using the so-called Ewald summation technique [35], which was originally developed in 1921 by Paul Peter Ewald (1888–1985) for calculating binding energies of crystals. Mathematically, the method consists of a division of the interaction into a screened short-range part which is calculated using a spherical cutoff, and a long-range part which is summed in reciprocal space, yielding a relatively fast convergence. Over the years, several algorithms have been developed that exhibit a better system size scaling behavior than the $\mathcal{O}(N^{3/2})$ scaling of the original Ewald method. The most popular of these are probably the $\mathcal{O}(N \log N)$ smooth particle mesh Ewald [36] and $\mathcal{O}(N)$ fast multipole [37] methods.

It was shown by de Leeuw et al. [38] in 1980 that, in addition to the explicit interparticle interactions, the infinite lattice is solvated by a surrounding dielectric continuum with permittivity ε_{sur}. This so-called surface energy depends on the total instantaneous dipole moment $M = |\mathbf{M}|$ of the simulation cell according to

$$\mathcal{U}_{surf} = \frac{2\pi}{(2\varepsilon_{sur} + 1)V} M^2. \tag{4.10}$$

Common choices of ε_{sur} are $\varepsilon_{sur} = 1$, ("vacuum boundaries") and $\varepsilon_{sur} = \infty$ ("tin-foil boundaries"). Furthermore, it has been shown [39] that it may be

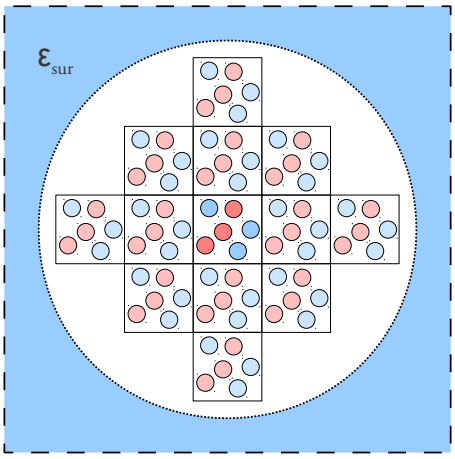

Figure 4.2: Illustration of periodic boundary conditions in two dimensions. The particles in the simulation cell interact with each other, as well with an infinite number of identical replicas of the simulation cell. In addition, the whole lattice is surrounded by a dielectric continuum of permittivity ε_{sur}.

beneficial in some cases to try to adjust ε_{sur} to match the dielectric constant of the simulated system. This, however, requires an *a priori* knowledge about the permittivity of the system under study, which is usually not accessible until after running the simulation.

In the context of crystals, for which the Ewald method was originally developed, the idea of imposing an infinite periodicity on the system is natural, whereas it is clearly an approximation for anisotropic systems such as fluids. For the simulation of a single solute such as a protein in a solvent bath, the PBCs will have the effect of increasing the effective solute concentration, sometimes to unphysical levels. Furthermore, the PBCs act to enhance or suppress the fluctuations of the simulated system due to the interaction between the instantaneous charge distribution in the central simulation cell and its identical copies. The artifacts induced by PBCs when simulating solvated biomolecules [40–43] and ionic systems [44–46] have been thoroughly investigated in the past, whereas their effect on the fluctuations in a dipolar bulk system is examined in Papers VI and VII.

Moving-boundary reaction field

A conceptually different way to mimic an infinite system is to apply a cut-off on the interparticle interactions, but approximating the fluid outside the cutoff sphere by a dielectric continuum with permittivity ε_{RF}. The surrounding continuum then produces a "reaction field" $\mathbf{E}_{RF}$ which solvates the total dipole $\mathbf{M}_{cut}$ of the cutoff sphere, according to

$$\mathbf{E}_{RF} = \frac{2(\varepsilon_{RF} - 1)}{\varepsilon_{RF} + 1} \frac{\mathbf{M}_{cut}}{r_{cut}^3}. \tag{4.11}$$

In the classical implementation by Barker and Watts [47], Eq. (4.11) is used in combination with toroidal boundaries, and thus the cut-off boundary is "mobile" in the sense that it is applied with respect to each individual particle in the system.

Compared to periodic boundary conditions, the moving-boundary reaction field scheme is easily implemented, especially since it can be simply reformulated as a modified pair potential. It, however, suffers from problems with discontinuities in energies and forces at the cutoff boundary, although this problem can be resolved by using suitable switching functions [24]. What is more surprising, and perhaps disturbing, is that this technique seems to suffer from exactly the same periodicity-induced artifacts as those obtained when using PBCs, in spite of not including any assumption of long-range periodicity. In Paper VI, we investigate this issue, even though the detailed explanation is still unclear.

Fixed-boundary reaction field

An alternative way to implement reaction field boundaries, originally proposed by Friedman [48] in 1975, is to use a *fixed* boundary between the molecular and continuum systems. This means that, rather than using toroidal boundary conditions, one encloses the simulated system with an appropriate, usually spherical, confining potential. By solving Poisson's equation under suitable boundary conditions [17], it can be shown that the effect of the dielectric continuum outside the boundary can be approximately described using so-called *image charges* (and, when appropriate, image dipoles), mimicking the reaction field from the surroundings. In this description, a charge of size q located at a point $\mathbf{r}$ with respect to the center of the simulation cell gives rise to an image charge of size

$$q^* = -\frac{\varepsilon_{RF} - 1}{\varepsilon_{RF} + 1}\frac{a}{r}q \tag{4.12}$$

located at

$$\mathbf{r}^* = \left(\frac{a}{r}\right)^2 \mathbf{r}, \tag{4.13}$$

i.e. outside the boundary of the simulation cell (see Figure 4.3). Thus, each particle interacts with all the $N - 1$ other particles inside the simulation cell as well as with the N image particles outside the simulation cell.

Naturally, the absence of toroidal boundaries means that there are no periodicity artifacts. However, by removing the toroidal boundaries one also introduces a physical surface into the system, which is unwanted when simulating a bulk system. In many of the studies carried out using these boundary conditions [49–51], the surface effects are found to have a relatively large impact on the structure and thermodynamics of the system, largely due to the non-isotropic orientation of molecules close to the confining surface. However, recent results [52] using a "hybrid" method that combines the image charge technique with toroidal boundaries indicate that these surface effects can be successfully eliminated. In Paper VIII, we combine Friedman's original method with suitably adjusted bias functions to minimize surface effects.

Hyperspherical boundary conditions

Another approach, originally developed by Caillol [53] in the early 1990's, is to confine the particles to the three-dimensional surface of a four-dimensional "hypersphere". This yields a closed space, thus avoiding surface effects without imposing any artificial periodicity to the system. The only caveat is that,

at least for small system sizes, there may be a significant curvature (in four dimensions) imposed on the three-dimensional space; the problem can be compared to the simulation of particles confined to the two-dimensional surface of a three-dimensional sphere. Although the method has not been given much attention in the past, possibly due to the mathematical rigor of the original papers, recent simulation results on large Stockmayer fluid systems [54] indicate that these boundary conditions may be a feasible alternative to periodic boundary conditions and reaction field methods.

4.4 Calculating dielectric constants

The dielectric constant of a dense fluid is a macroscopic property, in the sense that it depends strongly on the long-range structure of the material. Because of this, the task of developing analytical theories enabling the calculation of dielectric constants is tremendous for materials having even moderate ($\varepsilon \approx 20$) permittivities. One of the central formulas for the calculation of dielectric constants, as well as a large amount of other seminal work in dielectric theory, was developed by John G. Kirkwood (1907–1959) [55], and relates the dielectric constant to the magnitude of the fluctuations in the total dipole moment M of a (macroscopic) sample inside the infinite fluid:

$$\frac{(\varepsilon - 1)(2\varepsilon + 1)}{9\varepsilon} = \frac{\langle M^2 \rangle}{N} \frac{4\pi\rho}{9k_B T}. \tag{4.14}$$

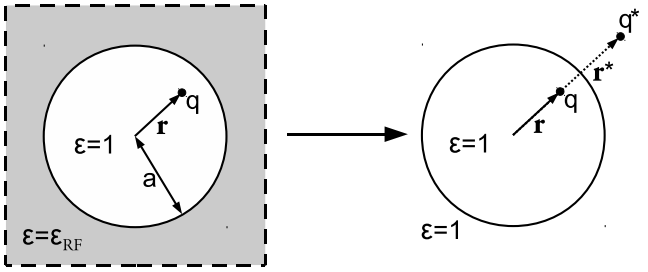

Figure 4.3: Schematic illustration of the fixed boundary reaction field technique. The response from the surrounding dielectric medium to a charge q can be described as the interaction with an imaginary "image charge" q^*, described by Eqs. (4.12) – (4.13).

In Eq. (4.14), the mean-square dipole moment $\langle M^2 \rangle$ quantifies the dipole fluctuations of the sample, N is the number of molecules contained in the sample, and ρ its number density. The quantity $\langle M^2 \rangle / N\mu^2$, where μ is the molecular dipole moment, is called the *Kirkwood factor* of the fluid and denoted by g_K. Equation (4.14) reduces the problem of obtaining ε to measuring or calculating $\langle M^2 \rangle$ for the particular fluid. The most draconian solution to this problem is to make the approximation $g_K = 1$ (or, equivalently, $\langle M^2 \rangle = N\mu^2$), amounting to ignoring the angular correlations between neighbouring dipoles. The so-called Onsager relation [13, 56] thus obtained however grossly underestimates ε for all but low-dielectric ($\varepsilon \leqslant 5$) materials [10]. Many less drastic approximations, primarily using integral-equation techniques, have also been applied, although neither of them seems to yield quantitatively reliable results for dielectric constants of strongly polar Stockmayer and dipolar hard sphere fluids [10, 23].

Given the apparently large difficulties in obtaining ε using analytical techniques, the natural choice is to instead use computer simulation techniques. This is however not obviously easier, given the unfortunate fact that ε is highly sensitive to long-range correlations of the fluid, which are difficult to describe accurately in a computer simulation because of the finite-size effects discussed in the previous section. Thus, the dielectric constant obtained from a computer simulation depends strongly on the choice of scheme for treating the long-range interactions. The issue of how to accurately calculate ε from a simulation therefore was a matter of some controversy in the late 1970's and early 1980's [57]. The issue was largely resolved, however, in 1983, when Neumann [58] derived fluctuation formulas applicable to a range of boundary conditions. In particular, he showed that Eq. (4.14) only holds when using periodic boundary conditions with $\varepsilon_{sur} = \varepsilon$, which is a rather unusual choice given the difficulties discussed previously. For the common choice of tinfoil boundaries ($\varepsilon_{sur} = \infty$), one should instead use the relation

$$\frac{(\varepsilon - 1)}{3} = \frac{\langle M^2 \rangle_\infty}{N} \frac{4\pi\rho}{9k_B T}, \tag{4.15}$$

where M in this context denotes the dipole moment of the whole simulation box.

Even though sampling the dipolar fluctuations is the most common way to calculate ε from a computer simulation, a few authors [59–61] have attempted to estimate ε through the response of the fluid to an externally applied field E_0. This approach is also closely related to the experimental definition of ε discussed in Section 2.3. From basic dielectric theory [13], we find the relationship

$$\langle \mathbf{M} \rangle / V = (\varepsilon - 1) E_0. \tag{4.16}$$

Thus, by sampling the mean value of the system dipole $\mathbf{M}$, which is nonzero in the direction of the applied field, an estimate of ε can be obtained. However, this procedure requires a careful adjustment of the field strength, since a too low value of $\mathbf{E}_0$ will lead to bad statistics in the sampling of $\mathbf{M}$, whereas increasing the field strength too much will lead to a saturation of the system polarization, yielding a too low value of ε. These issues, together with the fact that one "destroys" other equilibrium properties of the system by applying an external field, has lead to that this method for obtaining ε is less popular than measuring the dipolar fluctuations.

Even though calculating ε is not the main purpose in any of the papers included in the thesis, the Gaussian probability distributions discussed in Section 2.4 can be shown to be closely related to the fluctuation formulas [Eqs. (4.14) and (4.15)] used for the calculation of ε from a computer simulation. In Paper I, Eq. (2.15) is shown to yield a generalization of Eq. (4.14) to multipole moments higher than the dipole. Thus, by sampling a whole set of fluctuating multipole moments rather than just the dipole, one in principle creates a number of independent routes to obtaining ε. As is shown in Papers VI and VII, these methods are in many ways suboptimal for calculating the dielectric constant. However, they can provide useful tools for understanding the behavior of systems under periodic boundary conditions, as well as for investigating the nature of the dielectric approximation itself.

CHAPTER

FIVE

SUMMARY OF RESULTS

In this chapter, the main results from the eight papers included in the thesis will be briefly discussed. The organization of the papers into three separate sections follows the outline in Chapter 1.

5.1 Papers I–III: Electrostatic fluctuations

Paper I

In Paper I, the fluctuation formulas already discussed in Section 2.4 are derived by solving a standard dielectric boundary-value problem, i.e. by solving Poisson's equation under certain boundary conditions. The main results of the paper have already been given in Eqs. (2.13), (2.14), and (2.15), showing that (*i*) the probability distribution $P(M_\ell)$ of the axial 2^ℓ-pole moment of a dielectric sphere in a vacuum as well as in an infinite fluid is a Gaussian function, and (*ii*) the exponent α of the Gaussian function asymptotically (i.e., for large ε) goes as ε^{-1} inside an infinite fluid, whereas it is independent of ε for a dielectric sphere surrounded by vacuum. The formulas for $1 \leqslant \ell \leqslant 4$ are tested towards results from computer simulations of a weakly polar ($\varepsilon = 2.3$) Stockmayer fluid, yielding excellent agreement. Finally, an analysis of the free energy change A_ℓ^{solv} connected with the process of solvating the 2^ℓ-pole moment (see Figure 2.5) is carried out within a linear response approximation. The rather remarkable conclusions from this analysis are that (*i*) A_ℓ^{solv} is essentially independent of ℓ, and (*ii*) A_ℓ^{solv} is exactly independent of the radius R of the solvated sphere. Since there is in principle an infinite number of fluctuating multipole moments, the first conclusion implies that the total solvation free energy of a dielectric sub-volume in an infinite fluid is *infinite*,

regardless of ε and R. The origin of this unphysical divergence is discussed in qualitative terms, and it is shown how assigning a finite thickness δ, of molecular dimensions, to the discontinuity between the sphere and its surroundings yields a finite and reasonable free energy of solvation, as well as introducing a dependence of A_ℓ^{solv} on R.

In this context, we would also like to add that Eqs. (2.13), (2.14), and (2.15) were already derived by Scaife in a textbook [62] and in a Festschrift [63] before the submission of this manuscript. We sincerely apologize to the author for failing to acknowledge this before.

Paper II

In Paper II, we show how the solvation free energy A_{solv} of five different model systems can be treated in a general way using electrostatic fluctuation formulas together with Eq. (3.8). Some standard results from the literature, namely the solvation free energy of (*i*) a permanent dipole in an electric field, (*ii*) a dielectric sphere in an electric field, and (*iii*) a permanent dipole in a dielectric medium are re-derived in a straightforward manner. Furthermore, the cases of (*iv*) a polarizability in a dielectric medium and (*v*) a spherical sub-volume inside a dielectric medium (i.e., the system treated in Paper I), that cannot be treated using traditional mean-field techniques, are handled using the new approach. Since this approach is fully non-linear, the results for a dielectric sub-volume immersed in its own medium constitutes a generalization of the expressions for A_{solv} derived in Paper I. It is shown that the linear-response formalism taken there is indeed highly inaccurate for $\varepsilon > 5$, even though the divergence in A_{solv} still persists using a non-linear treatment. We also separate the energetic and entropic contributions to A_{solv}, showing that for a fluid where ε is independent of temperature, the driving force for solvation is purely entropic. Using parameters relevant for water at room temperature, however, yields energetic and entropic contributions of approximately equal magnitudes.

Paper III

In Paper III, electrostatic fluctuation formulas corresponding to those obtained in Paper I are derived for a spherical sub-volume inside a spherically confined fluid. Again, the properties of the dielectric model are obtained by solving an electrostatic boundary-value problem. This becomes significantly more complex than in the case of an infinite fluid due to the presence of dielectric discontinuities, and thus the resulting equations need to be solved numerically. Because of the inhomogeneity of the system, the magnitude of

the fluctuations, quantified through the inverse of the Gaussian exponent α, depends on (*i*) the position where M_ℓ is sampled, (*ii*) the radius R of the sampling sphere, and (*iii*) whether M_ℓ is sampled parallel or perpendicular to the confining surface. The results obtained from the dielectric model show that, in accordance with what one might expect, the effect of the surface is to effectively diminish the magnitude of the fluctuations. The effect is strongest for fluctuations perpendicular to the surface, and becomes significant when the distance between the surface of the sampling sphere and the confining surface is on the order of R. Finally, the dielectric continuum results are found to exhibit a quantitative agreement with results from MC simulations of a confined, strongly polar ($\varepsilon \approx 80$) Stockmayer fluid.

5.2 Papers IV–V: van der Waals interactions

Paper IV

In this paper we use the multipole fluctuation formulas from Paper I to calculate the fluctuation-driven electrostatic interaction between two spherical bodies of dielectric material. In the introduction of Paper IV, it is shown that this interaction exactly corresponds to the classical (Keesom) part of the van der Waals interaction. Due to the symmetry of the problem, or rather the lack thereof, the fluctuation formulas need to be generalized to include also the non-axial multipole components. To this end, the so-called spherical multipole moments $Q_{\ell m}$, defined through Eq. (21) of Paper IV, are employed. Schematically, the free energy of interaction between the two spheres is calculated by forming the joint probability distribution $P(Q_{1,\ell_1 m}, Q_{2,\ell_2 m})$, where indices 1 and 2 denote the respective sphere. The interaction free energy $A^{\text{int}}_{\ell m}(D)$, relative to infinite separation between the spheres, can then obtained by describing $P(Q_{1,\ell_1 m}, Q_{2,\ell_2 m})$ at infinite separation and at a finite separation D, according to

$$P(Q_{1,\ell_1 m}, Q_{2,\ell_2 m}; D \to \infty) = P(Q_{1,\ell_1 m})P(Q_{2,\ell_2 m}) \tag{5.1}$$

and

$$P(Q_{1,\ell_1 m}, Q_{2,\ell_2 m}; D) = P(Q_{1,\ell_1 m})P(Q_{2,\ell_2 m})e^{-\beta U_{\text{el}}(D)}, \tag{5.2}$$

where $U_{\text{el}}(D)$ denotes the electrostatic interaction between two instantaneous multipoles at a separation D. These relations are then used together with Eq. (3.8) to obtain $A^{\text{int}}_{\ell m}(D)$. To obtain the total interaction free energy, we sum up the contributions from different fluctuating multipoles, i.e.

$$A_{\text{int}} = \sum_{\ell=1}^{\infty} \sum_{m=-\ell}^{\ell} A^{\text{int}}_{\ell m}. \tag{5.3}$$

The numerical results from this approach are tested against the classical limit of Lifshitz theory, and the differences are found to be insignificant. The main motivation of the study is thus not to obtain new numerical results, but rather to give a new, and significantly simpler, derivation of the classical Lifshitz result.

Paper V

In Paper V, we compare the dielectric continuum results for $A_{\text{int}}(D)$ from Paper IV with results obtained for two interacting bodies of Stockmayer particles (see Figure 2.3) using a combined Monte Carlo simulation/perturbation theory approach. In practice, this means that *one* spherical cavity containing Stockmayer particles was simulated using the standard Metropolis algorithm, while saving a subset of the equilibrium configurations to disk. The distance-dependent interaction free energy between two such subsystems was then obtained by randomly selecting pairs from the set of saved configurations, translating them a distance D with respect to each other, and calculating $A_{\text{int}}(D)$ according to

$$A_{\text{int}}(D) = -k_B T \ln\langle e^{-\beta \mathcal{U}_{\text{int}}}\rangle_D, \tag{5.4}$$

where $\mathcal{U}_{\text{int}}$ is the interaction potential between two specific configurations of the spheres, and the subscript D indicates that the average is taken over all orientations of the subsystems having a fixed separation D.

The results are compared to the dielectric continuum results from Paper IV, and the agreement in $A_{\text{int}}(D)$ is found to be remarkably good down to separations on the scale of a particle radius. When comparing the individual contributions $A^{\text{int}}_{\ell m}(D)$ to the interaction free energy, however, we find that the dielectric model tends to overestimate the magnitude of the interaction compared to the Stockmayer model for $1 \leqslant \ell \leqslant 3$. This means that to get an agreement in the total interaction $A_{\text{int}}(D)$ there has to be an *under*estimation of the interaction magnitude for higher values of ℓ. We attribute this effect to interactions that are dominated by essentially single-particle interactions that are not handled well in the dielectric description. Finally, the interaction free energy is decomposed into its energetic and entropic contributions and compared to the dielectric model. In this case, there is a significant underestimation of the entropic penalty of correlating the fluctuations of the two spheres when using the dielectric continuum model. Once again, we attribute this to the neglect of the discrete nature of the fluid in the dielectric description.

5.3 Papers VI–VIII: Long-range corrections

Paper VI

In Paper VI, we investigate the effect of using periodic boundary conditions on the electrostatic fluctuations in a strongly polar Stockmayer fluid. Once again, the spherical multipoles $Q_{\ell m}$ are used for the analysis, and the magnitude of the fluctuations are quantified through the mean-square quantity $\langle Q_{\ell m} \rangle$. We find that the effect of the PBCs is to enhance (compared to in an infinite bulk system) the fluctuations of multipole moments of certain orientations, and equivalently to suppress other multipole components. This effect is attributed to the coupling between a permanent multipole $Q_{\ell m}$ and all its identical replicas in the simple cubic lattice, which can be either attractive, repulsive, or zero depending on its orientation described through ℓ and m. We corroborate this assumption by comparing the fluctuations of different multipole components to the reduced interaction tensors $S_{\ell m}$ (in Paper VI we use the notation $\widetilde{R}_{\ell m}$) describing the interaction between a unit multipole and all its periodic images. Finally, we make the corresponding comparison using the same model system instead simulated using a moving-boundary reaction field. Somewhat strikingly, we find essentially identical periodicity effects in this case, which we attribute to the use of toroidal boundaries.

Paper VII

The qualitative arguments from Paper VI are extended in Paper VII, where we develop a quantitative model relating the magnitude of multipole fluctuations to the effective interaction tensors $S_{\ell m}$. Furthermore, the analysis is extended to simulation cells having non-cubic geometries. The fluctuations are now quantified through a set of "apparent", m-dependent dielectric permittivities $\varepsilon_{\mathrm{PBC},\ell m}$. Using a straightforward electrostatic analysis we find that the anisotropic polarization induced by the PBCs yields a linear relationship between $\varepsilon_{\mathrm{PBC},\ell m}$ and $S_{\ell m}$, where the value of $\varepsilon_{\mathrm{PBC},\ell m}$ for $S_{\ell m} = 0$, obtained from a fitting of simulation data, coincides with the true dielectric constant $\varepsilon_{\mathrm{diel}}$ that the fluid would have without PBCs. The model also enables us to analyze the solvation energetics of the simulated systems. We find that the strong anisotropy in the dielectric constant is reflected in an anisotropic long-range solvation free energy of the fluid. However, when averaged over all different multipole orientations, the solvation free energy becomes very close to the desired value valid for an infinite isotropic fluid. We argue that this averaging effect explains the success of PBCs in reproducing reliable thermodynamic data for fluids, in spite of the unphysical periodicity present in the

method.

Paper VIII

In the final paper of this thesis, we implement the fixed-boundary reaction field method on the same Stockmayer model system as in Papers VI and VII. Since we are now simulating a spherical, non-periodic system, there are no periodicity effects on the fluctuating multipole moments. However, the use of a physical boundary separating the molecular system from the surrounding dielectric continuum induces a positional and orientational ordering close to the surface. We show how this can be fully remedied using suitable, self-adjusting bias functions that ensure a homogeneous distribution and isotropic orientation of particles inside the simulation cell. We furthermore find that the effect of the surface on the total system energy vanishes for strong enough couplings (i.e., short distances) between the molecular fluid and the surrounding dielectric medium. However, even with very strong couplings, a significant effect from the surface on the dielectric constant of the system still persists, manifesting itself through a suppression of electrostatic fluctuations when the radius of the sampling sphere approaches that of the simulation cell. Finally, we try to remedy this effect by assigning, somewhat unphysically, a negative dielectric constant $\varepsilon_{\mathrm{RF}}$ to the surrounding dielectric medium, meaning that the dielectric reaction field becomes *stronger* than the primary field inducing it. For strong enough reaction fields this partly solves the problem, although it is also shown to induce a ferroelectric phase transition of the fluid for high enough values of $\varepsilon_{\mathrm{RF}}$.

BIBLIOGRAPHY

[1] Franks, F. (ed.) (1972–82) *Water: A Comprehensive Treatise, Vols 1–7*. Plenum.

[2] Bagchi, B. (2005) Water dynamics in the hydration layer around proteins and micelles. *Chem. Rev.*, **105**, 3197–3219.

[3] Clark, G. N. I., Cappa, C. D., Smith, J. D., Saykally, R. J., and Head-Gordon, T. (2010) The structure of ambient water. *Mol. Phys.*, **108**, 1415–1433.

[4] Franks, F. (1981) *Polywater*. MIT Press.

[5] Davenas, E., et al. (1988) Human basophil degranulation triggered by very dilute antiserum against IgE. *Nature*, **333**, 816–818.

[6] Zheng, J., Chin, W.-C., Khijniak, E., Khijniak Jr., E., and Pollack, G. H. (2006) Surfaces and interfacial water: Evidence that hydrophilic surfaces have long-range impact. *Adv. Colloid Interface Sci.*, **127**, 19–27.

[7] Montagnier, L., Aïssa, J., Ferris, S., Montagnier, J.-L., and Lavallée, C. (2009) Electromagnetic signals are produced by aqueous nanostructures derived from bacterial DNA sequences. *Interdiscip. Sci. Comput. Life. Sci.*, **1**, 81–90.

[8] DeMeo, J. (2011) Water as a resonant medium for unusual external environmental factors. *Water*, **3**, 1–47.

[9] Teixeira, P. I. C., Tavares, J. M., and Telo da Gama, M. M. (2000) The effect of dipolar forces on the structure and thermodynamics of classical fluids. *J. Phys.: Condens. Matter*, **12**, 411–434.

[10] Stell, G., Patey, N., and Hoye, J. S. (1981) Dielectric constants of fluid models: Statistical mechanical theory and its quantitative implementation. *Adv. Chem. Phys.*, **48**, 183–328.

[11] Klapp, S. H. L. (2005) Dipolar fluids under external perturbations. *J. Phys.: Condens. Matter*, **17**, 525–550.

[12] Frenkel, D. and Smit, B. (2002) *Understanding Molecular Simulation*. Academic Press, second edn.

[13] Böttcher, C. J. F. (1952) *Theory of Electric Polarisation*. Elsevier, first edn.

[14] Evans, D. F. and Wennerström, H. (1999) *The Colloidal Domain: Where Physics, Chemistry, Biology and Technology Meet*. Wiley, second edn.

[15] Israelachvili, J. (1991) *Intermolecular & Surface Forces*. Academic Press, second edn.

[16] Griffiths, D. J. (1998) *Introduction to Electrodynamics*. Pearson Education, third edn.

[17] Jackson, J. D. (1999) *Classical Electrodynamics*. Wiley, third edn.

[18] Parsegian, V. A. (2006) *van der Waals Forces*. Cambridge University Press.

[19] Dzyaloshinskii, I. E., Lifshitz, E. M., and Pitaevskii, L. P. (1961) The general theory of van der Waals forces. *Adv. Phys.*, **10**, 165–209.

[20] Hill, T. L. (1988) *An Introduction to Statistical Thermodynamics*. Dover Publications.

[21] McQuarrie, D. A. (2000) *Statistical Mechanics*. University Science Books, second edn.

[22] Callen, H. B. (1985) *Thermodynamics and an Introduction to Thermostatistics*. Wiley, second edn.

[23] Hansen, J.-P. and McDonald, I. (2006) *Theory of simple liquids*. Academic Press, third edn.

[24] Allen, M. P. and Tildesley, D. J. (1989) *Computer Simulation of Liquids*. Oxford University Press.

[25] Metropolis, N., Rosenbluth, A. W., Rosenbluth, M. N., Teller, A. H., and Teller, E. (1953) Equation of state calculations by fast computing machines. *J. Chem. Phys.*, **21**, 1087–1092.

[26] Gubernatis, J. E. (2005) Marshall Rosenbluth and the Metropolis algorithm. *Phys. Plasmas*, **12**, 057303.

[27] Verlet, L. (1967) Computer "experiments" on classical fluids. I. Thermodynamical properties of Lennard-Jones molecules. *Phys. Rev.*, **159**, 98–103.

[28] Andersen, H. C. (1980) Molecular dynamics simulations at constant pressure and/or temperature. *J. Chem. Phys.*, **72**, 2384–2393.

[29] Nosé, S. (1984) A unified formulation of the constant temperature molecular dynamics methods. *J. Chem. Phys.*, **81**, 511–519.

[30] Hoover, W. G. (1985) Canonical dynamics: Equilibrium phase-space distributions. *Phys. Rev. A*, **31**, 1695–1697.

[31] Berendsen, H. J. C., Postma, J. P. M., van Gunsteren, W. F., DiNola, A., and Haak, J. R. (1984) Molecular-dynamics with coupling to an external bath. *J. Chem. Phys.*, **81**, 3684–3690.

[32] Steinbach, P. J. and Brooks, B. R. (1994) New spherical-cutoff methods for long-range forces in macromolecular simulation. *J. Comp. Chem.*, **15**, 667–683.

[33] Wolf, D., Keblinski, P., Phillpot, S. R., and Eggebrecht, J. (1999) Exact method for the simulation of Coulombic systems by spherically truncated, pairwise r^{-1} summation. *J. Chem. Phys.*, **110**, 8254.

[34] Fennell, C. J. and Gezelter, J. D. (2006) Is the Ewald summation still necessary? Pairwise alternatives to the accepted standard for long-range electrostatics. *J. Chem. Phys.*, **124**, 234104.

[35] Ewald, P. P. (1921) Die Berechnung optischer und elektrostatischer Gitterpotentiale. *Ann. Phys.*, **64**, 253–287.

[36] Essmann, U., Perera, L., Berkovitz, M. L., Darden, T. A., Lee, H., and Pedersen, L. (1995) A smooth particle mesh Ewald method. *J. Chem. Phys.*, **103**, 8577–8593.

[37] Greengard, L. and Rokhlin, V. (1987) A fast algorithm for particle simulations. *J. Comput. Phys.*, **73**, 325–348.

[38] de Leeuw, S. W., Perram, J. W., and Smith, E. R. (1980) Simulation of electrostatic systems in periodic boundary conditions. I. Lattice sums and dielectric constants. *Proc. R. Soc. Lond.*, **A 373**, 27–56.

[39] Boresch, S. and Steinhauser, O. (1997) Presumed versus real artifacts of the Ewald summation technique: The importance of dielectric boundary conditions. *Ber. Bunsenges. Phys. Chem.*, **101**, 1019–1029.

[40] Hünenberger, P. H. and McCammon, J. A. (1999) Effect of artificial periodicity in simulations of biomolecules under Ewald boundary conditions: A continuum electrostatics study. *Biophys. Chem.*, **78**, 69–88.

[41] Kastenholz, M. A. and Hünenberger, P. H. (2004) Influence of artificial periodicity and ionic strength in molecular dynamics simulations of charged biomolecules employing lattice-sum methods. *J. Phys. Chem. B*, **108**, 774–788.

[42] de Vries, A. H., Chandrasekhar, I., van Gunsteren, W. F., and Hünenberger, P. H. (2005) Molecular dynamics simulations of phospholipid bilayers: Influence of artificial periodicity, system size, and simulation time. *J. Phys. Chem. B*, **109**, 11643–11652.

[43] Reif, M. M., Kräutler, V., Kastenholz, M. A., Daura, X., and Hünenberger, P. H. (2009) Molecular dynamics simulations of a reversibly folding β-heptapeptide in methanol: Influence of the treatment of long-range electrostatic interactions. *J. Phys. Chem. B*, **113**, 3112–3128.

[44] Hummer, G., Pratt, L., and Garcia, A. (1998) Molecular theories and simulation of ions and polar molecules in water. *J. Phys. Chem. A*, **102**, 7885–7895.

[45] Hünenberger, P. H. (1999) Lattice-sum methods for computing electrostatic interactions in molecular simulations. Pratt, L. R. and Hummer, G. (eds.), *Simulation and Theory of Electrostatic Interactions in Solution*, vol. 492 of *AIP Conference Proceedings*, pp. 17–83.

[46] Bergdorf, M., Peter, C., and Hünenberger, P. (2003) Influence of cut-off truncation and artificial periodicity of electrostatic interactions in molecular simulations of solvated ions: A continuum electrostatics study. *J. Chem. Phys.*, **119**, 9129–9144.

[47] Barker, J. A. and Watts, R. O. (1973) Monte-Carlo studies of dielectric properties of water-like models. *Mol. Phys.*, **26**, 789–792.

[48] Friedman, H. L. (1975) Image approximation to the reaction field. *Mol. Phys.*, **29**, 1533–1543.

[49] Wallqvist, A. (1993) On the implementation of Friedman boundary conditions in liquid water simulations. *Mol. Simul.*, **10**, 13–17.

[50] Wang, L. and Hermans, J. (1995) Reaction field molecular-dynamics simulation with Friedman's image charge method. *J. Phys. Chem.*, **99**, 12001–12007.

[51] Petraglio, G., Ceccarelli, M., and Parrinello, M. (2005) Nonperiodic boundary conditions for solvated systems. *J. Chem. Phys.*, **123**, 044103.

[52] Lin, Y., Baumketner, A., Deng, S., Xu, Z., Jacobs, D., and Cai, W. (2009) An image-based reaction field method for electrostatic interactions in molecular dynamics simulations of aqueous solutions. *J. Chem. Phys.*, **131**, 154103.

[53] Caillol, J. M. (1992) Structural, thermodynamic, and electrical properties of polar fluids and ionic solutions on a hypersphere — theoretical aspects. *J. Chem. Phys.*, **96**, 1455–1476.

[54] Trulsson, M. (2010) Simulations of high-dielectric Stockmayer fluids in hyperspherical geometry. *J. Chem. Phys.*, **133**, 174105.

[55] Kirkwood, J. G. (1939) The dielectric polarization of polar liquids. *J. Chem. Phys.*, **7**, 911–919.

[56] Onsager, L. (1936) Electric moments of molecules in liquids. *J. Am. Chem. Soc.*, **58**, 1486–1493.

[57] de Leeuw, S. W., Perram, J. W., and Smith, E. R. (1986) Computer simulation of the static dielectric constant of systems with permanent electric dipoles. *Ann. Rev. Phys. Chem.*, **37**, 245–270.

[58] Neumann, M. (1983) Dipole moment fluctuation formulas in computer simulations of polar systems. *Mol. Phys.*, **50**, 841–858.

[59] Watts, R. O. (1981) Electric polarisation of water: Monte Carlo studies. *Chem. Phys.*, **57**, 185–195.

[60] Alper, H. E. and Levy, R. M. (1989) Computer simulations of the dielectric properties of water: Studies of the simple point charge and transferrable intermolecular potential models. *J. Chem. Phys.*, **91**, 1242–1251.

[61] Pegado, L. and Jönsson, B. Determining the dielectric permittivity of dipolar fluids in a slit simulation. Unpublished manuscript.

[62] Scaife, B. K. P. (1998) *Principles of Dielectrics*. Oxford University Press.

[63] Scaife, B. K. P. (1987) Multipolar fluctuations in a dielectric sphere. Barrett, T. W. and Pohl, H. A. (eds.), *Energy transfer dynamics: Studies and essays in honor of Herbert Fröhlich on his eightieth birthday*, Springer-Verlag.